JOURNAL OF AIRCRAFT
Vol. 37, No. 6, November–December 2000

Developing a Facility for Magnetoaerodynamic Experiments

J. S. Shang,* B. Ganguly,† R. Umstattd,‡ J. Hayes,§ M. Arman,¶ and P. Bletzinger**
Air Force Research Laboratory, Wright–Patterson Air Force Base, Ohio 45433-7913

Significant progress has been made in researching key components for a magnetoaerodynamic hypersonic experimental facility. A wind tunnel, which operates at a nominal Mach number of 6, has been restored to running condition and yielded preliminary data on aerodynamic drag and shock bifurcation for a jet spike. Plasma generation via radio-frequency (RF) radiation has also shown promise in providing a fairly uniform field around the RF-signal-carrying electrode. A technique for measuring temperature of weakly ionized air has been accomplished based on rotational spectra of vibrionic excitation of nitrogen. These newly acquired techniques are being integrated to create an interdisciplinary simulation facility.

Nomenclature

B = magnetic flux density
J = electrical current density
p = pressure
U = velocity vector, u, v, w
ρ = density
σ = electrical conductivity

I. Introduction

FOR most hypersonic flights the ionized air mixture within the shock layer frequently attains an electrical conductivity of 100 mho/m, depending on the flight speed and altitude.[1] The interaction of moving charged particles and an electromagnetic field will generate the Lorentz force as an additional mechanism to remove limitations imposed by conventional aerodynamic law. Resler and Sears[1] examined a dimensionless parameter governing the relative magnitude of the Lorentz and aerodynamic forces; it appears that the electromagnetic body force would become dominant at high altitude and high speed. These flow conditions naturally occur in hypersonic flight.

One of the possible uses of the Lorentz force is for acceleration or deceleration of gas continuously at subsonic and supersonic speeds without choking. This type of flowfield manipulation is achieved by the velocity and temperature coupling of electrically conducting media through Joule heating.[1,2] The flow orientation in a charged medium can also be altered by the intrinsic curvature of the trajectory of an electron traveling nonparallel to a magnetic field.[3] The Hall effect has been proposed by the aircraft industry as the driving force behind diverting charged fluid particles for combustion enhancement, as well as for inlet distortion and propulsive system weight reduction. Under some conditions the eddy current induced by the turbulent fluid particles crossing lines of magnetic induction will interact with the magnetic field and tend to damp turbulent motion. Even at moderate values of the Hartman number, the wall shear stress of turbulence can be reduced.[4]

The most outstanding aerodynamic phenomenon in a plasma field is that of compound wave propagation, shock-wave dispersion and bifurcation. A striking effect is the dramatically increasing standoff distance of a bow shock over a blunt body in a plasma field.[5,6] This effect was first predicted by the theoretical work of Bush[6] 40 years ago and then observed by Ziemer by applying a magnetic field to the hypersonic blunt-body flow.[5]

The research of shock-wave propagation in plasma was rejuvenated in Russia in the 1980s, the AJAX Concept,[7–10] and more recently by Ganguly et al.[11] Their collective findings can be summarized as the structure and the propagation speed of shock waves are significantly modified by nonequilibrium, weakly ionized gases. Therefore, if an electrically charged medium could be introduced upstream of the bow shock and the wave bifurcation quantified, these newly identified physical phenomena can have revolutionary potential for high-speed flight.

To introduce the plasma upstream of the shock wave, recent research tends to use either plasma injection or microwave energy deposition.[12–15] Some of the experimental results reported a drag reduction up to 50% or more, which raises the question of what is the main mechanism that produces this astonishing result. In principle, there are four basic mechanisms that can drastically alter the force exerted on a body: the jet spike that creates a bifurcation of the bow shock-wave structure; the nonequilibrium energy deposition among internal degrees of freedom; the purely thermal effect that simply increases the temperature of the oncoming airstream and effectively reduces the freestream Mach number; and finally, the electromagnetic effects in the form of the Lorentz force and Joule heating that change the Rankine–Hugoniot condition across the shock wave. It should become obvious, that a side-by-side experimental and computational interdisciplinary capability is absolutely necessary to address these presently unknown scientific issues.

The advent of high-performance computational technology has provided a rare opportunity to establish an interdisciplinary effort involving aerodynamics, electromagnetics, and chemical kinetics that was intractable just a few years ago. The validation and verification of computational magnetoaerodynamics, with regards to its fidelity to physics, are paramount for a new interdisciplinary field. The present approach is based on a side-by-side effort of computational and experimental techniques. First, the measurement will guide the mathematic formulation based on theory and provide a database for numerical replication. Then, for system risk reduction, both techniques will be applied to assess the engineering feasibility.

The present effort attempts to develop an experimental capability for magnetoaerodynamic hypersonics. The counterflow jet interaction with the bow shock wave at a Mach number of 5.8 is investigated to harness the most favorable interactions for hypersonic flight. The scientific findings in plasma generation and diagnostic procedure are verified and integrated into an interdisciplinary modeling and simulation capability to define the usable scope of aerodynamic and electromagnetic interactions. The challenge in the science issue alone warrants a redoubled effort; the impact to aerospace science is just too enormous to ignore.

Received 14 December 1999; presented as Paper 2000-0447 at the 38th Aerospace Sciences Meeting, Reno, NV, 10–13 January 2000; revision received 15 August 2000; accepted for publication 18 August 2000.

*Senior Scientist, Center of Excellence for Computational Simulation. Fellow AIAA.
†Research Scientist, Propulsion and Power Directorate.
‡Research Scientist, Captain USAF, Direct Energy Directorate.
§Aerospace Engineer, Air Vehicles Directorate.
¶Research Scientist, Direct Energy Directorate.
**Visiting Scientist, Propulsion and Power Directorate.

II. Technical Approach

The gist of the present research initiative is to develop a basic experimental research program to discover and to validate magnetoaerodynamic phenomena for hypersonic simulation technology. The interaction of a weakly ionized gas with an applied magnetic field is investigated under a controlled environment. The experimental facility consists of a blowdown, high-Reynolds-number wind tunnel, plasma generators, and mostly nonintrusive diagnostic instrumentation. The high-Reynolds-number wind tunnel was designed to simulate a flow condition at a nominal Mach number of 6.0, at the stagnation temperature 610 K, and a range of stagnation pressure of 0.69–14 MPa. The simulated freestream pressure therefore has a range from 4–77 torr (0.5–10.0 kPa). This facility can sustain a testing period up to 10 min and is the main test bed for the present research program.

Two methods of plasma generation have been used; one method is based on radio-frequency (RF) radiation from an antenna. In this design the nose capsule of a blunt body is used as the source, and the electric circuit is equipped with a tuner to match the impedance of the power source and load. An RF signal emitted with sufficient intensity will ionize the ambient air adjacent to the blunt body for plasma generation. The other method of plasma generation adopts the conventional dc discharge, which has an obviously unique feature of being macroscopically time independent. Both methods are designed to generate a fairly uniform plasma with an electron density around $10^{10}/cm^3$ over a pressure range from 4–10 torr.

To monitor the level of ionization and stability of the plasma, plasma diagnostics are required. The electron density of the plasma field is measured by microwave interferometry, mutual inductance coils, and will be verified by a Langmuir probe. Another important parameter is the thermodynamic properties of the plasma field. The gas mixture temperatures is measured by a spectral analysis of the emission of the molecule. From these data and the electromagnetic field information, the electrical conductivity can be ascertained. All of the aforementioned data can be used to verify and calibrate the computed species concentration based on the finiterate chemical kinetic model including the master equation for translational-vibrational transition.

The present basic research program consists of three phases. In phase one the Mach 6 tunnel was restored to running condition and recalibrated to assess the flowfield condition. In phase two the selected plasma generator and all required diagnostic tools were integrated into the wind-tunnel data acquisition system. In phase three the research effort was concentrated on improving the measurement accuracy and data generation. In the experimental program the electric charge separation across the shock wave and the transient behavior of the internal degree-of-freedom energy deposition downstream of the shock wave is planned. In both cases the thermodynamic and electromagnetic states across the shock were investigated. The quantification of the weakly ionized gas composition, electron density, electrical conductivity, and current density has been attempted.

Once all of the transport properties of the weakly ionized gas are ascertained, the Rankine–Hugoniot jump condition modified by an applied electromagnetic field can be quantified. An applied magnetic field up to 0.5 T has been generated by a solenoid coil embedded within the test model. The aerodynamic force and the energy required for the plasma generation were measured for assessing the engineering feasibility in high-speed flight.

III. Description of Wind Tunnel

The Mach 6 wind tunnel has been restored to running condition. Several recalibrating tests were successfully accomplished. A research effort for a force balance model design and the provision of a solenoid coil was also completed. Now the wind tunnel has passed a safety recertification. A thorough system shakedown was also accomplished before the plasma generator installation.

In Fig. 1 Mach-number distributions along the centerline of the tunnel are given. The data were collected at the distance of 25.4–254 mm from the nozzle exit plane at four measure stations. The Mach-number distributions at three stagnation pressures 6.89×10^2, 1.37×10^3, and 2.68×10^3 kPa are presented. The stagnation temperature is maintained at a constant value of 610 K for all cases studied. The maximum difference in deduced Mach numbers at all measure conditions is less than 2%. The maximum scattering is confined within the domain bounded by the nozzle exit plane to a distance of 127 mm downstream. In essence, the axial flow gradient is negligible, and the operational Mach number of this tunnel is determined to be 5.80.

The available test core of the blowdown jet at the stagnation pressure of 6.89×10^2 kPa is depicted in Fig. 2. In general, the jet core has a nominal diameter of 203.2 mm, but the radial dimension of the jet is actually contracting by a factor of 1.13 from the nozzle exit plane to a distance of 254 mm downstream. The most uniform Mach-number distribution is located at a distance of 203.2 mm downstream of the nozzle exit plane. At this location the available jet core also reduces to a diameter of 160.2 mm.

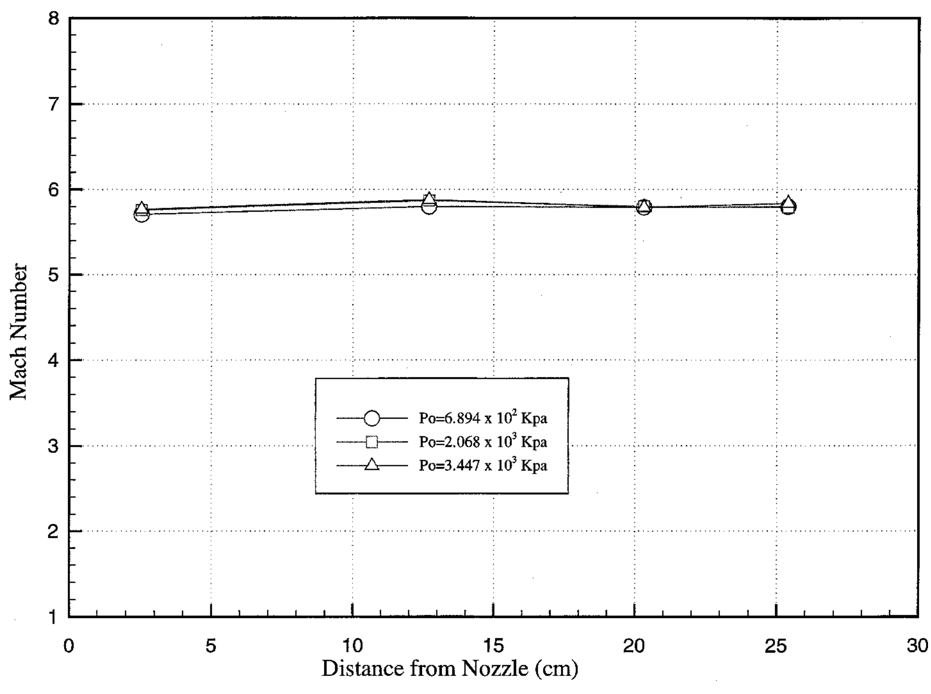

Fig. 1 Mach-number distributions along tunnel centerline.

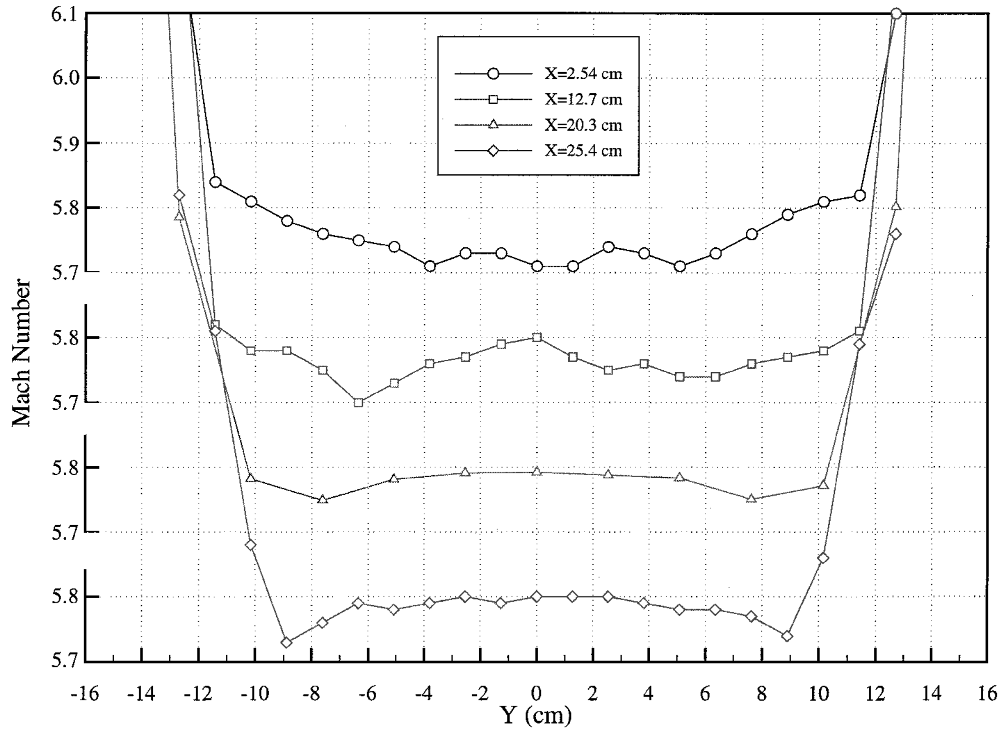

Fig. 2 Mach-number distributions across tunnel walls.

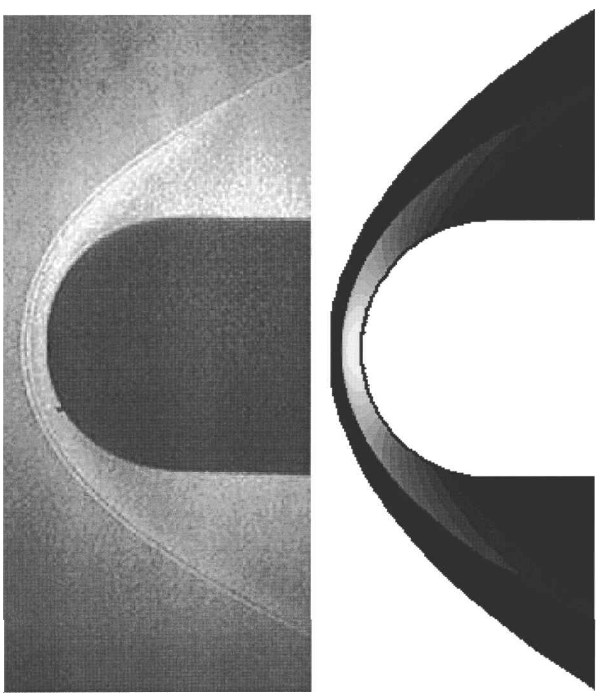

Fig. 3 Comparison of bow-shock-wave structure of a hemispherical blunt body at Mach 5.80.

As a calibration of the wind tunnel and an assessment of blockage interference, schlieren photographs of bow shock waves over a blockage model were collected at the four survey locations. The hemispherical blockage model has a nose radius of 38.1 mm and merged continuously to the cylindrical afterbody. The blockage model is mounted on a retractable stem support in the testing chamber. The flowfield of the test section was also monitored by the static pressure gauge; no discernible blockage interference was detected.

Figure 3 presents a comparison of the schlieren photograph and the density contours of calculated results. The numerical result is generated on a (50 × 40) mesh system under the identical experimental stagnation condition $T_0 = 610$ K and $P_0 = 6.889 \times 10^2$ kPa. The comparison of experimental and computational results shows overall agreement of the entire flowfield. Both results show an essentially normal shock wave at the stagnation region followed by a rapid expansion around the shoulder of the blunt nose. Specifically, the standoff distance of the experimental observation agrees well with calculation and correlated data.[16] The data yield a standoff distance $\Delta/R = 0.157$ in comparison with the correlated value by Ambrosio and Wortman (Ref. 16), $\Delta/R = 0.153$ and the calculated value of $\Delta/R = 0.146$.

IV. Plasma Generation

Presently, the phenomena of nonequilibrium energy deposition,[17,18] shock-wave dispersion, and bifurcation[10,11,19,20] in a plasma field have been identified as the most uncertain science issues. A more recent study by Josyula[21] using the master equation to evaluate the nonequilibrium vibration-translation transition has shown that the energy deposition indeed can increase the standoff distance by lowering the density in the shock layer, but the Rankine–Hugoniot condition is unaltered by the energy deposition process. On the other hand, the effect of the electromagnetics can definitely modify the Rankine–Hugoniot condition across a shock.[1,3] The general normal shock relation for a plasma can be derived for a shock wave parallel to the x coordinate. The jump condition of a normal shock wave becomes[19,20]

$$
\begin{aligned}
[\rho u] &= 0 \\
[p + \rho u^2] &= \int (J_y B_x - J_z B_y)\,\mathrm{d}x \\
[\rho u v] &= \int (J_z B_x - J_x B_z)\,\mathrm{d}x \\
[\rho u w] &= \int (J_x B_y - J_y B_x)\,\mathrm{d}x \\
[\rho u H] &= \int J^2/\sigma\,\mathrm{d}x \\
[B_x] &= 0 \\
[J_y/\sigma - w B_x + u B_x] &= 0 \\
[J_x/\sigma - u B_y + v B_x] &= 0
\end{aligned}
\qquad (1)
$$

where H denotes the total enthalpy of the flow, and the parameters contained within the square brackets indicate the end states across the shock wave. The preceding jump conditions will be reduced to that derived by Sutton and Sherman[3] if the plasma has a perfect electrical conductivity and the Hall current is negligible. Under these conditions $J = \boldsymbol{k}(\mathrm{d}B_y/\mathrm{d}x) - \boldsymbol{j}(\mathrm{d}B_z/\mathrm{d}x)$ holds, and the resultant jump conditions are obtained by a straightforward integration with respect to x

$$
\begin{aligned}
[\rho u] &= 0\\
[p + \rho u^2] &= -\left[\left(B_y^2 + B_x^2\right)/\, 2\mu\right]\\
[\rho u v] &= [B_x B_y]\\
[\rho u w] &= [B_x B_z]\\
[\rho u H] &= \left[\, - u\left(B_y^2 + B_x^2\right)/\, 2\mu + B_x(v B_y + w B_x)/\mu\right]\\
[B_x] &= 0\\
[u B_x - w B_x] &= 0\\
[v B_x - u B_y] &= 0
\end{aligned}
\tag{2}
$$

where μ is the magnetic permeability of the plasma. The basic effect of an electromagnetic field on a shock wave rests on two additional entropy change mechanisms.[19,20] One of them is the Joule heating, which is positive and will contribute to an entropy increase across the shock. On the other hand work can also be performed by the electromagnetic forces on the moving gas particles. Depending on the polarity of the induced or applied electromagnetic field, the total entropy for the open system can be reduced.[19,20] As a direct consequence of entropy reduction, the wave drag of the shock wave will diminish. This physical phenomenon may be singled out by immersing a bow shock wave in a plasma medium. For an electromagnetic shock tube this controlled environment is easily achieved.[5] For a conventional wind tunnel generating a plasma field upstream of a enveloping shock wave presents a serious challenge.

A critical choice in the present experimental effort is the appropriate mechanism to introduce plasma upstream of the enveloping shock. A key concern also rests on the practical implementation to flight vehicles in the future. Two approaches are considered for the drag-reduction investigation; one of which is the commonly adopted plasma injection.[12−15] In the injection process the plasma is introduced to the flowfield by a counterflow jet stream. The interaction of the counterflow jet with the freestream is much more complex than recognized, but the plasma inclusion is also not straightforward. Another approach is to study the effect of the Lorentz force on the standoff distance of the bow shock wave. To meet this objective, a fairly uniform plasma field must envelop the blunt body. An RF plasma source is chosen over a dc discharge.[22] In fact the RF plasma generation is not treated as an antenna problem but as a RF-carrying electrode and ambient ground plane.[23,24] Under this arrangement at a given RF power setting and a ambient pressure, the RF signal produces a plasma discharge between the electrode and a nearby ground plane. It was discovered in our preliminary research that at pressure range above 1 torr it was not possible to localize the discharge between electrodes at an RF power level of 1 kW. Instead, the discharge completely envelopes the surface of the signal-carrying electrode, which is a desired feature for the present experiment.

Figure 4 presents the glow discharge over the hemispherical cylinder in a vacuum chamber at an ambient pressure of 8 torr. Under this test condition a nearly uniform and steady plasma sheath was maintained over the entire surface of the hemispherical nose. The plasma is generated at a frequency of 13.56 MHz corresponding to a free-space wavelength of 22 m. In the vacuum chamber and after the initial plasma ignition, the power required to sustain the plasma generation is bracketed between 150 to 475 W. However in the test section of the tunnel the power requirement is anticipated to increase as a result of the inelastic collisions with the oncoming air mixture at a temperature of 78 K. Additional electronic density enhancements have been accomplished by installed dc discharging diodes.

The present RF plasma generation process also has drawbacks. First, the plasma generation process is inefficient. Much of the RF power dissipates as resistive heating on the surface of electrode;

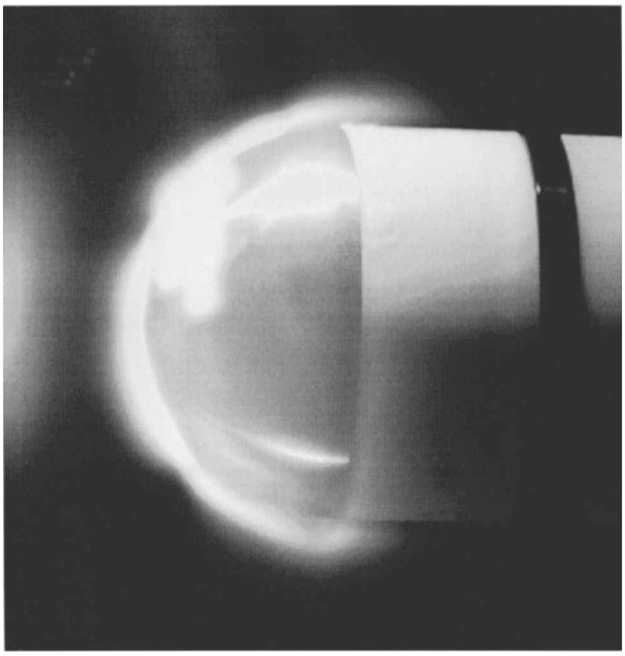

Fig. 4 Glow discharge from an RF-signal-carrying electrode.

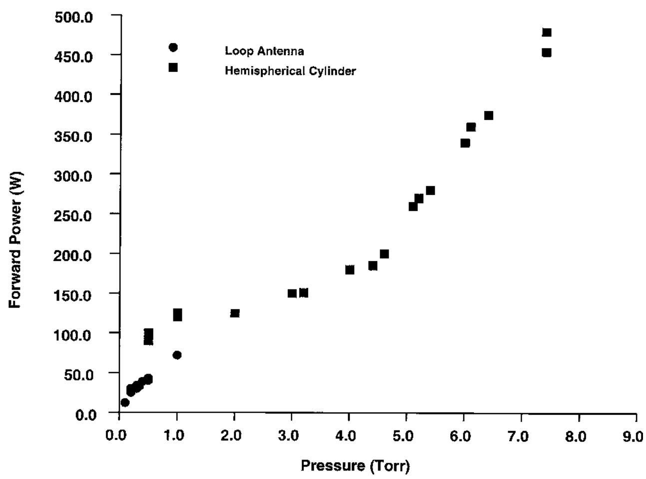

Fig. 5 RF breakdown of electrodes.

only a fraction of the power actually feeds the plasma generation process. Second, the resistive heating of the electrode, which is the blunt-body model in the present application, will prevent any meaningful heat-transfer measurement on the model. Nevertheless, the RF power requirement as determined in the vacuum chamber is depicted in Fig. 5. In this figure the power requirement for a loop antenna is also included. The loop antenna generated a fairly uniform plasma at the 1 torr pressure with 100 W of RF input and a reflected power of less than 2%. These data reflect the fact that the 13.56 MHz RF operating frequency is compatible with electron-neutral collision frequencies from 10 to 100 MHz for maximum energy transfer from RF to an electron. This collision frequency regime corresponds to neutral pressure around 1 torr. It provides an indication that the efficiency of energy conversion can be improved by using a higher-frequency source for plasma generation in a higher-pressure environment.

V. Flowfield Diagnostics

The understanding and quantification of a shock in plasma will require knowledge of some properties of the plasma and neutral air mixture in the wind tunnel.[25] Two critical parameters for the present experiment are the internal-degree-of-freedom gas temperatures and the electrical conductivity or, at least, the electron density of the self-sustained plasma. In terms of the level of technical challenge, the determination of transport properties of a plasma medium is more than equal to that of plasma generation. In addition to the unknown thermally nonequilibrium state of the weakly ionized air mixture, the measurements of nonisotropic electron density, magnetic permeability, and electric resistivity of the plasma medium are extremely uncertain.[17−19]

At present, four measuring methods are under consideration for determining the electron density of the plasma. First, the direct impedance measurement of the plasma field has given a global order-of-magnitude evaluation. Then the microwave interferometry, Langmuir probe, and reflectometry will be attempted. The preference of using one technique over the other depends on the plasma generation method and the accessibility of a beam path from a microwave transmitter to a receiver.[11] In view of these available choices, the electron density measurement technique is still presently under intensive study.

The investigation of accuracy and reliability of gas temperature measurement is derived from the rotational line shape fitting of N_2 plasma, which involves plasma-induced emission from the second positive electronic transition $C^3\Pi_u$ to $B^3\Pi_g$ (Ref. 25). Three different vibration transitions have been measured to ensure measurement accuracy and repeatability. The rotational temperatures are obtained from contour analyses of the spectra because the individual rotational quantum state are not resolvable as a result of the complexity of the spectra. In Fig. 6 the measured and calculated spectra are shown for a 3 torr discharge. The plasma emission is measured with a charge coupled device (CCD) detector array with a 400-ms time constant.

In Fig. 7 the measured rotational temperatures are plotted as a function of the discharge current for a N_2 plasma at a pressure of 10 torr. The measurements are collected for three different vibrational bands by the radially averaged emission. This plot also exhibits the temperature estimates from the on-axis and the end-view emission measurements. The fitted gas temperature revealed a data scattering ±40 K at the gas temperature of 800 K. The discrepancy between the two sets of data are incurred by the radiation trapping of the low J lines or of the low rotational quantum number. This conclusion was also supported by the current dependent axial electrical field measurement. The present results also show that a careful analysis of several vibrational bands along with a data fit for only high J lines is needed. The gas temperature measurement accuracy can be ensured by comparing plasma-induced emission of several vibrational manifolds.

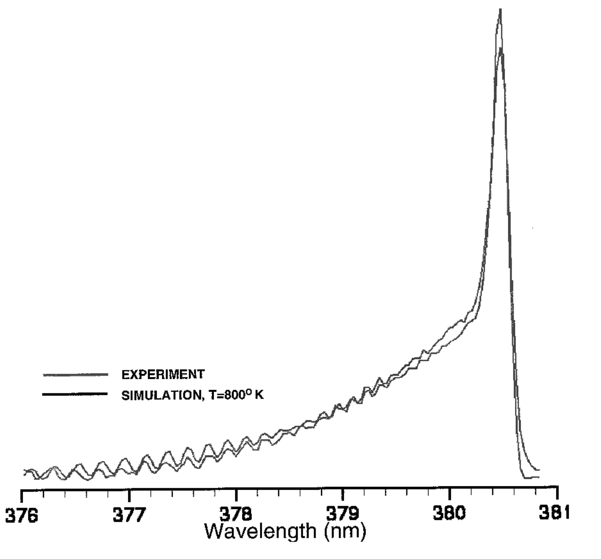

Fig. 6 Comparison of N_2 lamp CCD camera image.

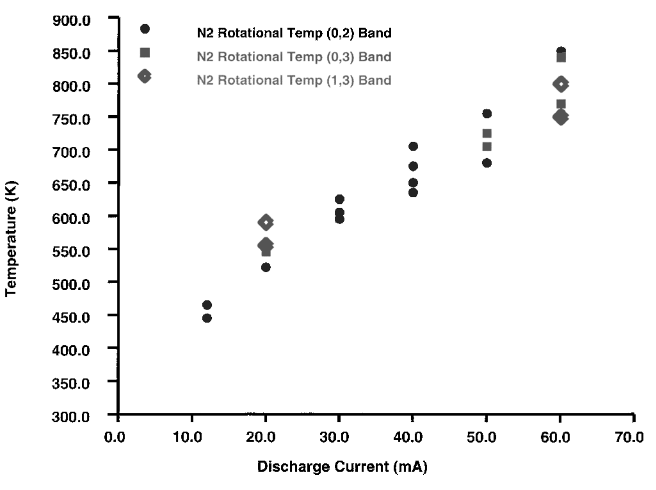

Fig. 7 Temperature vs discharge current (10 torr).

VI. Jet-Spike Bifurcation

Most experiments of wave drag reduction in a plasma field were accomplished by injection.[13−15] Some intricate ideas of energy deposition using nonintrusive mechanism were also put forward.[26] A common feature of these demonstrations was hinged on the interaction of the supersonic stream with the introduced flowfield perturbation. As a consequence of local flow adjustment to the counterflow jet, a rather complex shock-wave system was formed and eventually led to wave drag reduction. This mechanism of wave drag reduction was completely independent of the electromagnetic forces. All sources of drag reduction resulting from plasma injection were not well understood, and therefore a quantification of the drag reduction contributed by each mechanisms was not possible. The present investigation attempts to address mainly the issue of counterflow jet and its interaction with the bow shock. A preliminary testing program is focused on the jet-spike bifurcation.

The wave drag reduction in aerodynamic applications by either a spike or a jetspike on a blunt-nosed body is well known.[27−30] The wave drag reduction of the present investigation is derived from the splitting of a single strong shock wave into multiple and sequential shock waves. Even if the total pressure rise across the multiple and sequential shock waves is identical to that of a single shock wave, the entropy jump across the multiple wave system is much less. This difference is based on the fact that the entropy jump across each shock wave is nonlinear and is proportional to the cubic power of pressure jump. The spike-nosed blunt body enveloped by multiple shocks will thus encounter lower wave drag. However, if the injection pressure range is lower than the bifurcation point, a unsteady motion is oberved to induce large amplitude oscillations through shock bifurcation.

According to experimental results of Malmuth et al.[15] at the Mach-number range from 2.0 to 4.0, the greatest drag reduction occurred in the moderate long penetration mode.[15] However, in the present experiment at Mach number of 5.8, the maximum drag reduction is found at the shock bifurcation point. In the present work no effort was placed on the optimization of the jet spike from the blunt body to achieve the maximum wave drag reduction. At the identical injection mass rate and stagnation pressure, the most effective way to reduce drag is observed by nozzle design to achieve the maximum jet penetration. The potential gain from the jet-spike optimization is demonstrated by the following comparison of two different counterflow jet streams.

Both injections were emitted from the stagnation point of a blunt body with a hemispherical nose radius of 38.1 mm. At the jet stagnation temperature of 294.4 K and stagnation pressure of 1.0295×10^3 kPa, both the jets have the same amount of mass flow $m = 0.097$ kg/s from the identical sonic throat 2.38 mm in diameter. The ratio between tunnel and jet stagnation pressure is $p_j / p_o = 1.5$. One of the models has a sonic exit with an axial velocity component of 341 m/s. The schlieren photograph of this jet spike is depicted in Fig. 8. The jet of the other model is generated by a slender conical nozzle with an area ratio of four between the exiting plane and sonic throat $A_{\text{exit}} / A^* = 4.0$, and the jet exit Mach number is 2.94. The schlieren photograph of the supersonic jet spike is given in Fig. 9.

From Figs. 8 and 9 the basic features of the sonic and supersonic counterflowing jets are similar. Both jets are terminated by a Mach disk downstream of the bow shock wave. The jet stream stagnates

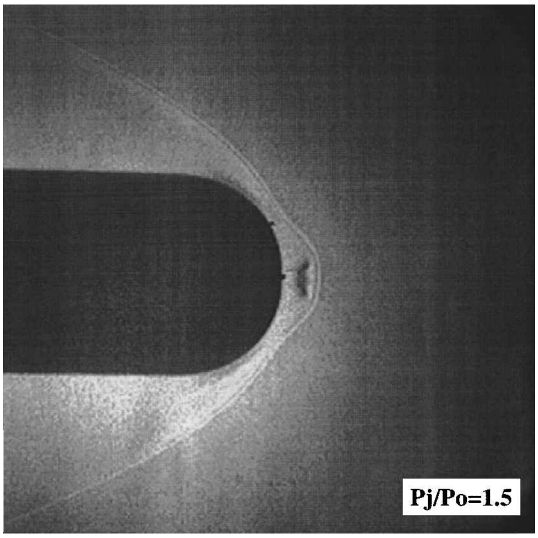

Fig. 8 Shock formation of sonic jet spike.

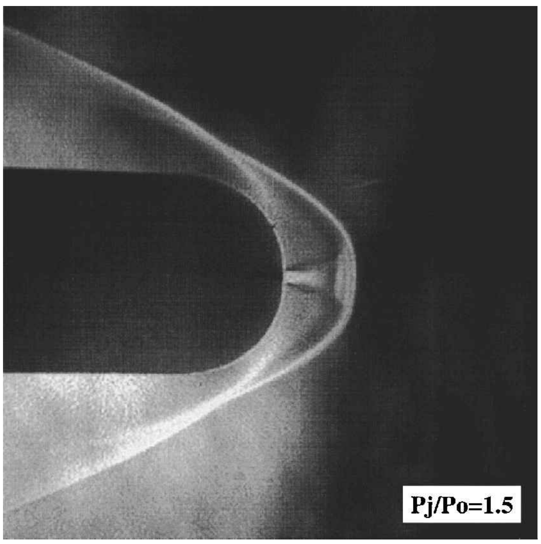

Fig. 9 Shock-wave formation of a supersonic jet spike.

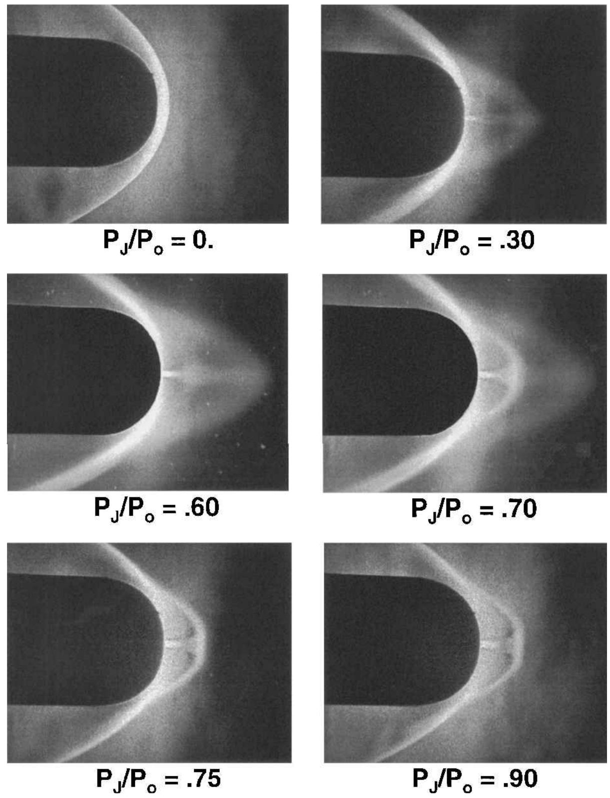

Fig. 10 Jet-spike shock bifurcation.

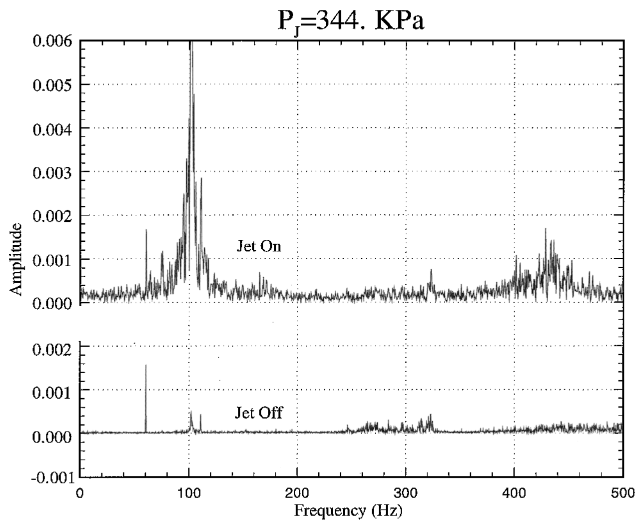

Fig. 11 Spectral data of drag measurements.

along the axis of symmetry producing a free stagnation point between the Mach disk and the bow shock and significantly modifying the enveloping bow shock wave. The jet then reverses its direction to appear as a free shear layer and reattaches upstream to the shoulder of the hemispherical cylinder. The reattachment process creates a circumferential stream deflection from the blunt nose and induces a ring shock. The main difference in flowfield structures between the sonic and supersonic jet is the penetration length. Unfortunately, the sonic jet model was not instrumented for aerodynamic force measurement, thus no detailed comparison of wave drag reduction is possible.

The unsteady flowfields of spike and jet spike of a blunt body were noted a long time ago.[27–30] These self-sustained oscillations have been observed for a wide variety of shear-layer impingement phenomena.[31] The highly organized oscillatory fluid motions are sustained by feedback or upstream pressure propagation through the subsonic free shear layer and by a selective disturbance amplification of the fluctuations through the shear layer. The spike-tipped buzz phenomenon even exhibits aerodynamic bifurcation when the length of the spike is extended or retracted from the blunt body to a critical value.[29,30] An identical aerodynamic bifurcation for the jet spike is also detected.

The observed aerodynamic bifurcation is depicted in Fig. 10. Six schlieren photographs are included at a tunnel stagnation condition of $T_0 = 610$ K and $P_0 = 6.889 \times 10^2$ kPa. Each photograph represents the six different jet stagnation pressure settings and is identified by the normalized value with respect to the tunnel stagnation condition p_j / p_0. The flowfield becomes unsteady even at the lowest injection pressure level of 0.148. As the jet stagnation pressure increases, the length of jet penetration upstream increases accordingly. Because of the unsteady aerodynamic motion, the image of the jet induced shock wave in the schlieren photograph becomes blurred by multiple exposures. Meanwhile the amplitude of oscillatory motion is also increased until it reaches the maximum around $p_j / p_0 = 0.7$. At this point a bifurcation of shock-wave structure takes place; further increase in jet stagnation pressure does not alter the complex shock structure significantly.

The spectral data of the oscillatory drag force sensor under the testing condition are presented in Fig. 11. For the preliminary investigation the spectral data were recorded up to 500 Hz. Only two typical data sets are included in the presentation, one of them describes the oscillatory motion when the jet spike is near the bifurcation.

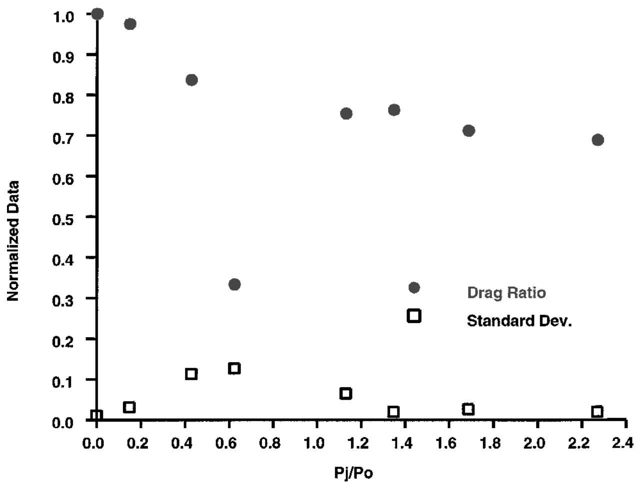

Fig. 12 Drag measurements of jet-spike bifurcation.

At this changing dynamic state at least two dominant frequencies around 100 and 440 Hz are easily detected. The standard deviation of drag measurement at this critical state grows rapidly by a factor of 11.72 relative to the no-injection condition.

In Fig. 12 the drag force measured by three prestressed load cells at eight different jet stagnation conditions is given. The flowfield is generated with stagnation conditions of $T_0 = 610$ K and $P_0 = 6.889 \times 10^2$ kPa. Three load cells were used to record the total aerodynamic force along the body axis. The force measuring model is mounted on a model support strut in such a manner that only the axial component of the aerodynamic force can be sampled. The measured data contain solely the total axial force exerted on the entire model, including the wave drag, skin-friction drag, base drag, and the reverse thrust of the counterflow jet.

A meaningful presentation of the drag data is accomplished by plotting the drag ratio normalized by the measured drag force without the jet spike—the baseline case. It is observed that even at the lowest jet injection pressure the measured drag is lower than the baseline case. The data indicate that the drag reduction caused by shock-shape modification completely overwhelms the reverse thrust by the jet spike. The drag reduces to merely 34% of the baseline case at the shock bifurcation. The drag ratio maintains at the level of 70% of the baseline case for jet stagnation pressures as high as 2.25 times of the tunnel stagnation condition $p_j / p_0 = 2.25$.

The standard deviation of the fluctuating drag measurements also consistently reaffirms the earlier observation that after the injection pressure exceeds the critical value the jet-spike induced unsteadiness diminishes. From the preliminary drag measurement a 30% drag reduction is realizable by a jet spike at Mach number 6 for a hemispherical blunt body.

VII. Conclusions

Progress has been made in the attempt to develop a wind tunnel for magnetoaerodynamic experiments. The probe survey of the Mach 6 tunnel exhibits a repeatable performance within a 2% data scattering band. Plasma generation via an RF electrode at 13.56 MHz shows promise in generating a fairly uniform plasma field adjacent to the blunt-body model. The rotational emission spectra fitting technique for gas temperature measurement demonstrate an accuracy of 5%.

The preliminary jet-spike bifurcation experiment reveals a critical state for steady fluid motion. The control parameter is the stagnation pressure ratio between the oncoming stream and the counterflow jet. When the counterflow jet is generated by a sufficiently high stagnation pressure, a steady motion can be maintained.

The drag reduction for a blunt body generated by a cold counterflow jet in steady flow field reaches an asymptote of 30% of the blunt-body flow without injection. The drag reduction near the bifurcation has a value as high as 68.9%. The present finding suggests a rigorous reexamination of drag reduction procedures using energy deposition techniques.

Acknowledgments

The research team deeply appreciates the sponsorship by S. Walker of the Air Force Office of Scientific Research. The invaluable contributions by R. Peterkin, Jr., Scott Harris, Eswar Josyula, and the wind-tunnel crew; Hank Baust, Joe Martin, Tom Norris, Ray Raber, Glenn Williams, Sam Price, and Michael Green are duly acknowledged. The computing effort was supported in part by a grant of HPC time from the Department of Defense High Performance Computing Shared Resource Centers at Wright–Patterson Air Force Base.

References

[1]Resler, E. L., and Sears, W. R., "The Prospects for Magneto-Aerodynamics," *Journal of Aerospace Science*, Vol. 25, April 1958, pp. 235–245, 258.

[2]Meyer, R. C., "On Reducing Aerodynamic Heat-Transfer Rates by Magnetohydrodynamic Techniques," *Journal of Aerospace Science*, March 1958, pp. 561–566, 572.

[3]Sutton, G. W., and Sherman, A., *Engineering Magnetohydrodynamics*, McGraw–Hill, New York, 1965, pp. 285–339.

[4]Mitchner, M., and Kruger, C. H., *Partially Ionized Gases*, Wiley, New York, 1973, pp. 163–241.

[5]Ziemer, R. W., "Experimental Investigation in Magneto-Aerodynamics," *American Rocket Society Journal*, Vol. 29, Sept. 1959, pp. 642–647.

[6]Bush, W. B., "Magnetohydrodynamic-Hypersonic Flow Past a Blunt Body," *Journal of Aerospace Science*, Vol. 25, Nov. 1958, pp. 685–690.

[7]Novichkov, N., "Russia in the Forefront of Aerospace Technology," *Military Parade*, May/June 1994, pp. 68–71.

[8]Gurijanov, E. P., and Harsha, P. T., "AJAX: New Directions in Hypersonic Technology," AIAA Paper 96-4609, Nov. 1996.

[9]Mishin, A. P., Bedin, N. I., Yushchenkova, G. E., and Ryazin, A. P., "Anomalous Relaxation and Instability of Shock Waves in Gases," *Soviet Physics—Technical Physics*, Vol. 26, 1981, pp. 1363–1368.

[10]Mishin, G. I., "Shock Waves in a Weakly Ionized Nonisothermal Plasma," *Soviet Technical Physics Letters*, Vol. 11, March 1985, pp. 112–114.

[11]Ganguly, B. N., Bletzinger, P., and Garscadden, A., "Shock Wave Damping and Dispersion in Nonequilibrium Low Pressure Argon Plasma," *Physics Letters*, Vol. 230, July 1997, pp. 218–222.

[12]Cain, T., and Boyd, D., "Electroaerodynamics and the Effect of an Electric Discharge on Cone/Cylinder Drag at Mach 5," AIAA Paper 99-0602, Jan. 1999.

[13]Ganiev, Yu. Ch., Gordeev, V. P., Krasilnikov, A. V., Lagutin, V. I., Otmennikov, V. N., and Panasenko, A. V., "Theoretical and Experimental Study of the Possibility of Reducing Aerodynamic Drag by Employing Plasma Injection," AIAA Paper 99-0603, Jan. 1999.

[14]Bityurin, V. A., Velikodny, V. Yu., Klimov, A. I., Leonov, S. B., and Potebnya, V. G., "Interaction of Shock Waves with a Pulse Electrical Discharge," AIAA Paper 99-3533, June–July 1999.

[15]Malmuth, N. D., Fomin, V. M., Maslov, A. A., Fomichev, V. P., Shashkin, A. P., Korotaeva, T. A., Shipyuk, A. N., and Pozdnyakov, G. A., "Influence of a Counterflow Plasma Jet on Supersonic Blunt Body Pressures," AIAA Paper 99-4883, Nov. 1999.

[16]Ambrosio, A., and Wortman, A., "Stagnation Point Shock Detachment Distance for Flow Around Spheres and Cylinder," *American Rocket Society Journal*, Vol. 32, 1962, p. 281.

[17]Adamovich, I. V., and Rich, W., "The Effect of Superelastic Electron-Molecule Collisions on the Vibrational Energy Distribution Function," *Journal of Physics D: Applied Physics*, Vol. 30, 1997, pp. 1741–1745.

[18]Candler, G. V., and Kelley, J. D., "Effect of Internal Energy Excitation on Supersonic Air Flow," AIAA Paper 99-4964, Nov. 1999.

[19]Shang, J. S., "An Outlook of CEM Multidisciplinary Applications," AIAA Paper 99-0336, Jan. 1999.

[20]Shang, J. S., Canupp, P. W., and Gaitonde, D. V., "Computational Magneto-Aerodynamic Hypersonics," AIAA Paper 99-4903, Nov. 1999.

[21]Josyula, E., "Computational Study of Effect of Oxygen Atoms on Vibrationally Relaxation of N_2 in High Speed Air Flow past Blunt Body," AIAA Paper 99-4835, Nov. 1999.

[22]Lowry, H., Stepanek, C., Crosswy, S. P., Smith, M., Price, L., Ruyten, W., and Felderman, J., "Shock Structure of a Spherical Projectile in Weakly Ionized Air," AIAA Paper 99-0600, Jan. 1999.

[23]Umstattd, R., Pi, T., Luhmann, N., Jr., Scheitrum, G., Caryotakis, G., and Miram, G., *Plasma Deposition of Oxide Cathodes, High Energy Density Microwaves*, edited by R. Phillips, American Inst. of Physics, Woodbury, NY, 1999, pp. 280–288.

[24]Arman, M. J., "Plasma Filled Radial Acceleration," *Advances in High Power Microwave Sources and Technologies*, Inst. of Electrical and Electronics Engineers (to be published).

[25] Herzberg, G., *Molecular Spectra and Molecular Structure. 1. Spectra of Diatomic Molecules*, Van Nostrand, New York, 1950, pp. 127–253.

[26] Riggins, D. W., Nelson, H. F., and Johnson, E., "Blunt Body Wave Drag Reduction Using Focused Energy Deposition," *AIAA Journal*, Vol. 37, No. 4, 1999, pp. 460–467.

[27] Finley, P. J., "The Flow of a Jet from a Body Opposing a Supersonic Free Stream," *Journal of Fluid Mechanics*, Vol. 26, Pt. 2, 1966, pp. 337–368.

[28] Bogdonoff, S. M., and Vas, I. E., "Preliminary Investigations of Spiked Bodies at Hypersonic Speeds," *Journal of Aerospace Science*, Vol. 26, Feb. 1959, pp. 65–74.

[29] Shang, J. S., Hankey, W. L., and Smith, R. E., "Flow Oscillations of Spike-Tipped Bodies," *AIAA Journal*, Vol. 20, No. 1, 1982, pp. 25, 26.

[30] Calarese, W., Shang, J. S., and Hankey, W. L., "Investigation of Self-Sustained Shock Oscillations on a Spike-Tipped Body at Mach 3," *Proceedings of the American Society of Mechanical Engineers' Winter Annual Meeting*, 1981, pp. 151–156.

[31] Shang, J. S., and Hankey, W. L., "Numerical Simulation of Self-Excited Oscillations in Fluid Flows," *The Series on Recent Advances in Numerical Methods in Fluid*, Vol. 3, edited by W. G. Habashi, Pineridge, Swansen, Wales, U.K., 1984, pp. 543–582.